

Transport of carbon dioxide in linear low-density polyethylene determined by permeation measurements and NMR spectroscopy

M.F. Laguna, J. Guzmán, E. Riande*

Instituto de Ciencia y Tecnología de Polímeros (CSIC), 28006 Madrid, Spain

Received 31 May 2000; received in revised form 26 September 2000; accepted 31 October 2000

Abstract

This work reports the transport of carbon dioxide in compression molded linear low-density polyethylene films. A common characteristic of the transport is that the curves that depict the dependence of the permeability coefficient of CO₂ on the upstream pressure exhibit a sharp increase in the low pressure region as the upstream pressure decreases at moderately high temperatures. This behavior can be explained by assuming that absorption and adsorption processes govern the transport of CO₂ in the films. The dual mode parameters calculated for co-extruded and compressed films are compared. The diffusion coefficient of CO₂ in the films is also obtained using NMR techniques. The value of the diffusion coefficient is nearly one order of magnitude higher than that determined from permeation measurements. The possible reasons for this discrepancy are discussed. © 2001 Elsevier Science Ltd. All rights reserved.

Keywords: Polyethylene films; NMR spectroscopy; Permeation measurements

1. Introduction

Gas transport in films involves solution of the gas in the film, diffusion through it, and desorption of the gas on the other face of the film. Micro-Brownian motions of the chains in rubbery materials may provide the source of the penetrant-scale hole needed for diffusion. In most cases, the performance of films in the rubbery state is excellent as far as their permeability is concerned, but it is poor with regard to their selectivity characteristics. For this reason, glassy instead of rubbery membranes are used for separation processes.

The presence of crystalline entities in rubbery films such as poly(ethylene) may alter the permeability of the films as a consequence of an increase in the tortuosity of the diffusive path caused by the crystallites and/or a decrease of solubility in the crystalline regions. The crystallites also reduce the mobility of the chains close to the anchoring points in the crystals. Moreover, annealing that contributes to the thickening of the crystals at expenses of the crystalline–amorphous interface may affect gas transport in semi-crystalline rubbery films.

Earlier work carried out on gas transport through co-extruded linear low-density polyethylene LLDPE films revealed some unexpected facts [1,2]. For example, the increase in permeability observed in co-extruded LLDPE

films after annealing is not due to changes in the diffusion coefficient (in fact this parameter slightly diminishes with annealing), but to a significant increase in the apparent solubility coefficient. On the other hand, the permeability coefficient of the films sharply increases at rather low upstream pressures [3], dependent on temperature and the nature of the penetrant.

A goal of this work is to investigate the transport of CO₂ in LDDPE films obtained by compression in order to learn whether co-extrusion is responsible for the differences observed in gas transport in these membranes when compared with gas permeation in rubbery membranes. For this purpose the permeation characteristics of CO₂ in LLDPE films were measured under different upstream pressures.

On the other hand, in the determination of the diffusion coefficient from permeation measurements, the concentration of the penetrant is not homogenous across the sample. NMR techniques may provide the means to measure the diffusion coefficient at constant concentration. By using this technique, Cain et al. [4,5] found that the translational diffusion coefficient of CO₂ in poly(dimethyl siloxane) has a wide distribution. Analysis of these results led these authors to conclude that the fraction of molecules of CO₂ compatible with the diffusion coefficient obtained from permeation measurements is rather small. In this work the diffusion coefficient of CO₂ in LLDPE films was also measured using NMR techniques with the aim of investigating how

* Corresponding author.

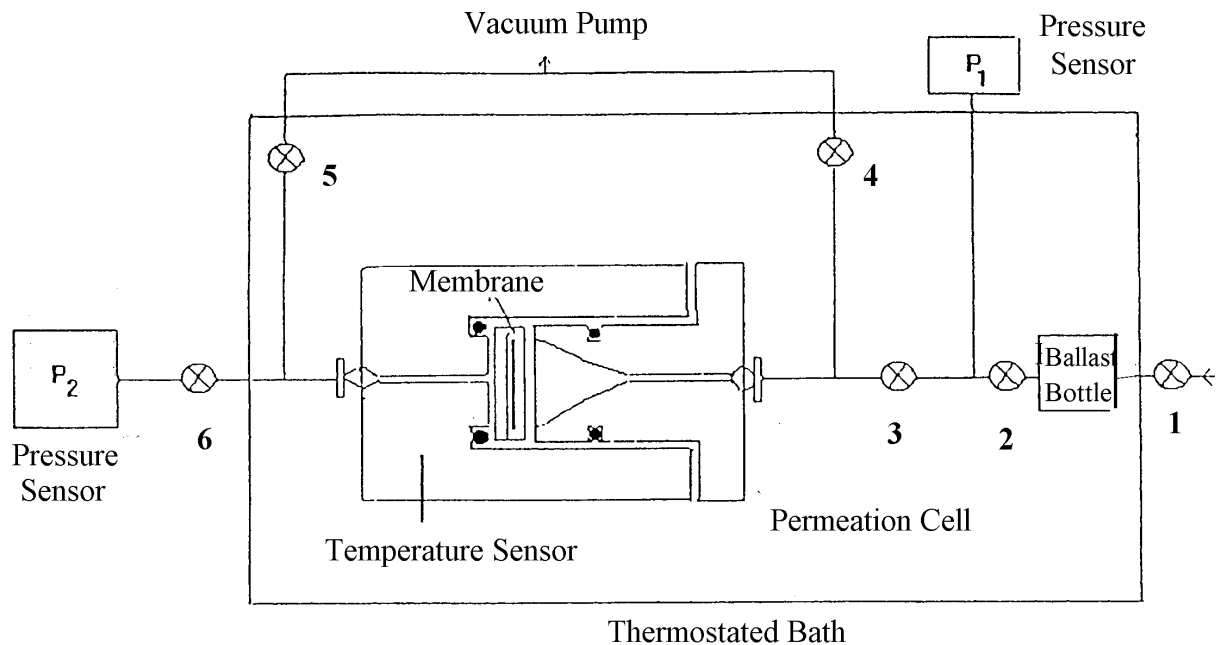


Fig. 1. Set-up for gas transport measurements.

the value of D thus obtained compares with that determined from permeation measurements.

2. Experimental part

2.1. Characteristics of the LLDPE films

Pellets of a copolymer of 1-octene-*co*-ethylene (Dow LLDPE, $\rho = 0.902 \text{ g cm}^{-3}$), with roughly 8% content of 1-octene, were pressed between two hot plates to obtain films of $276 \pm 7 \mu\text{m}$. The thermograms of the films, determined with a DSC-7 Perkin–Elmer calorimeter at a heating rate of $20^\circ\text{C min}^{-1}$, present a melting endotherm that extends from 47 to 110°C with the maximum of the peak

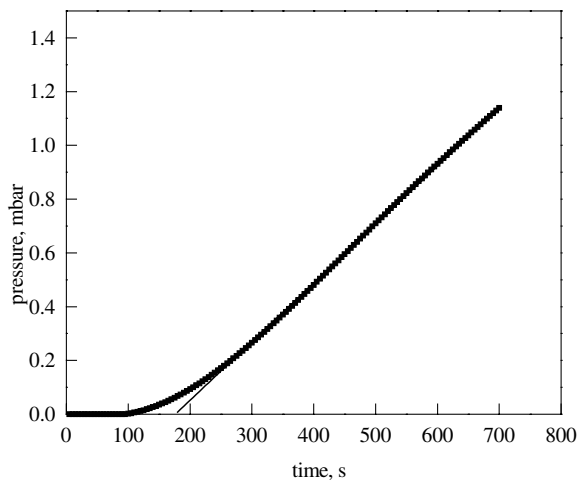


Fig. 2. Illustrative plot showing the evolution with time of the pressure of CO_2 in the downstream chamber at $p = 676.4 \text{ cm of Hg}$ and $T = 25^\circ\text{C}$.

located at 99°C . The degree of crystallinity of the film, obtained from the melting endotherms by assuming that the melting enthalpy is 290 J g^{-1} was 0.26.

2.2. Permeation measurements

The permeation of CO_2 in LLDPE films was measured in the experimental device shown in Fig. 1. Keeping valves 3, 4, 5 and 6 open and valve 2 closed, high vacuum ($\sim 10^{-4} \text{ mbar}$) was made for 48 h in both the upstream and downstream chambers separated by the film. Then valves 4 and 5 were closed, valve 2 was opened and the CO_2 kept in a ballast bottle placed inside the thermostated bath, at a pressure close to that used in the experimental, flowed into the high pressure chamber. Taking zero as the time at which valve 2 was opened, the variation of the pressure with time in the downstream chamber was detected with a pressure sensor. Before each experiment, the leak curve was determined by measuring the variation of the pressure with time in the downstream chamber in vacuum.

2.3. NMR techniques

The dynamics of CO_2 in LLDPE was studied in a Bruker MSL-300 spectrometer using the spin echo technique. After removing the air in a tube containing small pieces of pellets of LLDPE inside, CO_2 at 9 atm of pressure was let in. The tube was closed in situ and the experiment was performed at 25°C .

To identify the relation between the gradient in Gauss cm^{-1} and the value that the set-up shows, the apparatus was previously calibrated by measuring the diffusion coefficient of a liquid of known diffusion coefficient, such as benzene ($D = 2.21 \times 10^{-5} \text{ cm}^2 \text{ s}^{-1}$).

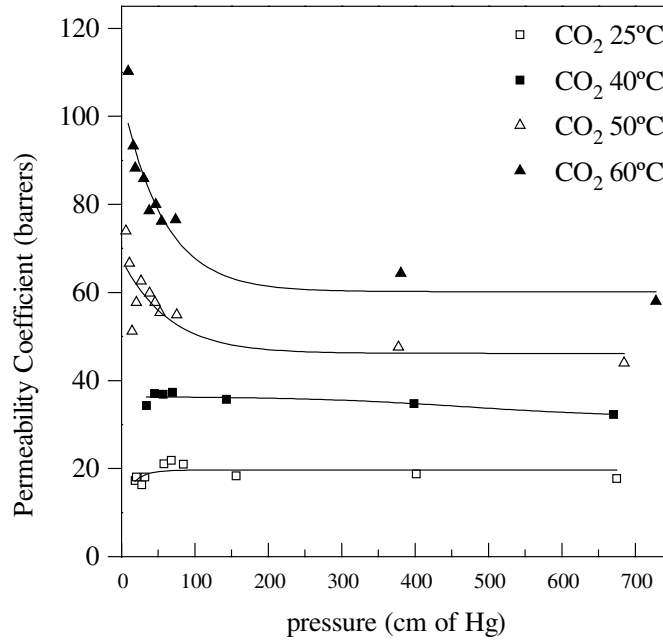


Fig. 3. Variation of the permeability coefficient of carbon dioxide with the pressure of the upstream chamber at several temperatures.

2.4. Permeation results

An illustrative curve depicting the evolution with time of the pressure, p , in the downstream chamber is shown in Fig. 2. The curve presents at short times a transitory followed at longer times by a steady state region in which p is a linear function of t . The permeation curve in the whole time domain can be obtained by integrating Fick’s second law using the appropriate boundary conditions. In the steady state region, the amount of gas $Q(t)$ diffusing at time t is given by [6,7]

$$Q(t) = \frac{DC_h}{l} \left(t - \frac{l^2}{6D} \right) \tag{1}$$

where C_h is the gas concentration in the high pressure

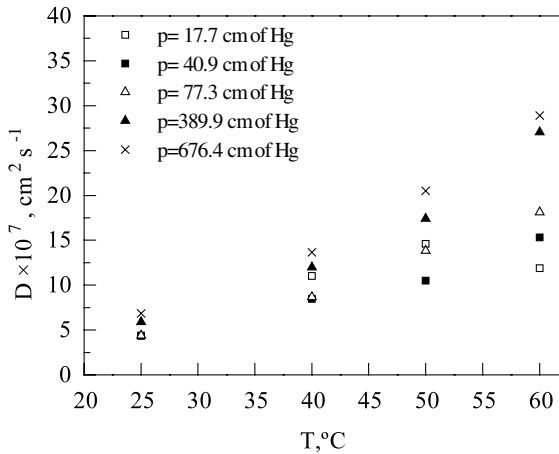


Fig. 4. Variation of the diffusion coefficient of carbon dioxide with temperature for different values of the upstream pressure.

chamber, l the film thickness and D is the apparent diffusion coefficient. In steady state conditions, the flow of gas through a membrane can be written as

$$J = -P \frac{p_l - p_h}{l} \cong P \frac{p_h}{l} \tag{2}$$

where P is the permeability coefficient and p_h and p_l are, respectively, the pressures of the gas in the upstream and downstream chambers. From Eq. (2) the following expression is obtained for the permeability coefficient:

$$P = \frac{273}{76} \left(\frac{Vl}{ATp_h} \right) \left(\frac{dp}{dt} \right) \tag{3}$$

where V is the volume of the low pressure chamber, A the effective film area, p_h the pressure of the gas in the high pressure chamber, p the pressure of the low pressure chamber and T is the absolute temperature of the thermostat. The unit used to express the permeability coefficient is the Barrer ($=10^{-10} \text{ cm}^3 \text{ (STP) cm cm}^{-2} \text{ s cm of Hg}$).

The diffusion coefficient can be obtained from $Q(t)$ by the lag method suggested by Barrer [8]

$$D = \frac{l^2}{6\theta} \tag{4}$$

where θ , the time lag, can be determined from the intercept of $p(t)$ on the time axis.

Values of the permeability coefficient for CO_2 are plotted as a function of the upstream pressure, at different temperatures, in Fig. 3. It can be seen that at 50 and 60 °C, the values of the permeability coefficient undergo a sharp increase with decreasing p_h , in the low-pressure region. This upturn is not detected in the isotherms corresponding to 25 and 40 °C in the range of pressures studied.

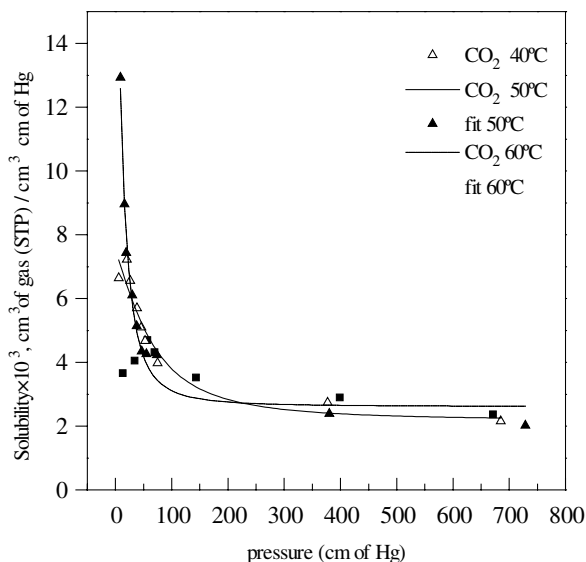


Fig. 5. Isotherms showing the variation of the solubility coefficient of carbon dioxide with the up-stream pressure at the temperatures indicated.

Results for the apparent diffusion coefficient of CO₂ for different upstream pressures are plotted as a function of temperature in Fig. 4. The curves show that the diffusion coefficient increases with increasing temperature and, in most cases, D tends to augment as the upstream pressure goes up.

The apparent solubility coefficient, S , is usually defined as

$$S = P/D \quad (5)$$

Values of the apparent solubility coefficient calculated from Eq. (5) are plotted as a function of the upstream pressure, at 40, 50 and 60°C, in Fig. 5. It can be seen that the resulting curves, at each temperature of interest, exhibit the same pattern as that shown by the permeability coefficient. Thus S decreases as p_h increases, and in the region of low upstream pressures the solubility coefficient experiences a sharp increase with decreasing values of p_h . It is worth noting that the increase occurring in the values of S is larger with increasing temperature.

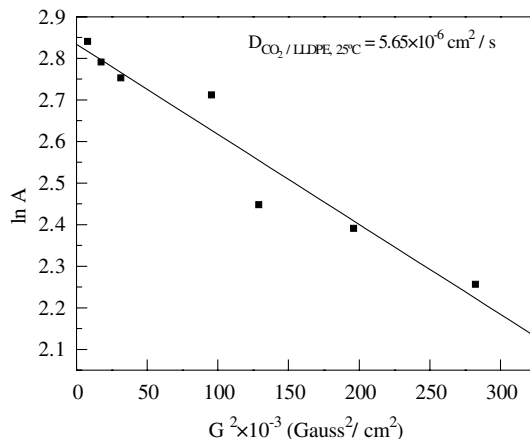


Fig. 7. Plot of $\ln A(G)$ versus G^2 for system CO₂/polyethylene at 25°C and 676.4 cm Hg of pressure.

2.5. NMR results

The sorbed molecules of CO₂ in the polymer matrix continuously change their spatial locations. In an inhomogeneous magnetic field, the component of the displacement in the direction of the field gradient changes the Larmor frequency of nuclear spins attached to the diffusing molecules. The amplitude of the spin echo is reduced as the molecules diffuse to greater distances during the interval τ between the pulses. The spin echo method is based on the difference between the amplitude of the echo with and without a field gradient G applied for a time δ . With the pulse sequence [9,10] shown in Fig. 6 the spin echo amplitude in the presence of a gradient $A(G)$ is given by

$$A(G) = A(0) \exp[-(\gamma G \delta)^2 D(\Delta - \delta/3)] \quad (6)$$

where $A(0)$ is the amplitude without gradient, γ the gyromagnetic ratio of the nucleus, Δ the diffusion time, G the gradient (Gauss cm⁻¹), δ the time that the gradient is applied and D is the diffusion coefficient. The values of δ and Δ used in the spin echo sequence were 5×10^{-3} and 15×10^{-3} s. The correspondence between G in Gauss cm⁻¹ and G in arbitrary units was obtained by calibration with

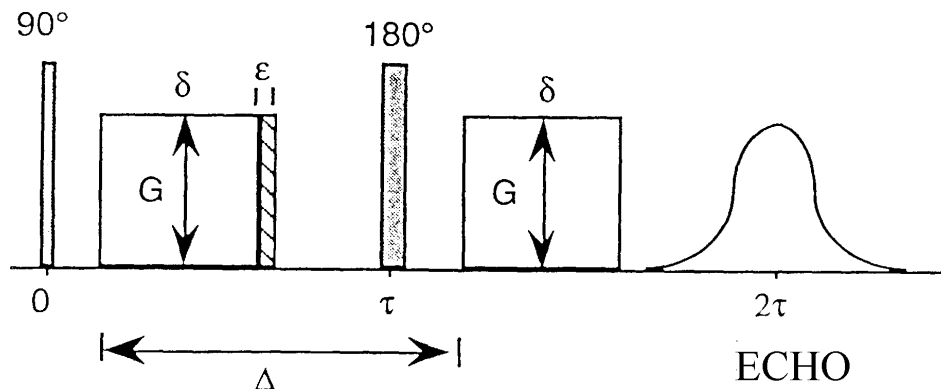


Fig. 6. Pulsed-gradient spin echo scheme.

Table 1
Values of the individual parameters for CO₂ associated with the first and second modes of transport

T (°C)	b (cm Hg) ⁻¹	$10^3 \times k_D$ cm ³ of gas (STP)/(cm ³ of polymer cm Hg)	C'_H cm ³ gas(STP)/cm ³ of polymer
40	0.03	2.2	0.23
50	0.08	2.1	0.18
60	0.45	2.1	0.12

benzene, using the value of 2.21×10^{-5} cm² s⁻¹ reported for the diffusion coefficient of this compound.

Values of $A(G)$ for CO₂ in LLDPE were obtained for different values of G , at 9 atm of pressure. The plot $\ln A(G)$ against G , shown in Fig. 7, was fitted to a straight line from whose slope the value of 5.65×10^{-6} cm² s⁻¹ was obtained for the diffusion coefficient of CO₂.

3. Discussion

The solubility coefficient of gases in rubbery films can be predicted by using the Flory–Huggins equation that accounts for the mixture of the gas in the liquid form with the polymer [11]. The value of S thus obtained is given by [12]

$$\ln S = -\ln \bar{V}_A - (1 + \chi_A) + (1 + 2\chi_A)\bar{V}_A C_A - \frac{\lambda_{bA}}{RT_{bA}} \left(1 - \frac{T_{bA}}{T}\right) = \ln k_D + bC_A \quad (7)$$

where \bar{V}_A and C_A are, respectively, the partial molar volume and the concentration of the penetrant A , λ_{bA} and T_{bA} denote, respectively, the molar latent heat and the boiling point of A , and χ_A is the enthalpic interaction parameter between the penetrant and the polymer. Eq. (7) reduces to Henry's equation at low concentrations and deviates positively from it at high concentrations. According to Eq. (7), the more condensable a gas is, the more soluble the gas in a rubbery membrane is. This prediction, however, is not borne out by the results of Fig. 5 where it can be seen that the solubility coefficient of CO₂ in LLDPE films decreases with increasing pressure.

On the other hand, the diffusion process depends on the interaction coefficient ζ between the penetrant and the polymer matrix. By assuming that ζ is governed by the fractional free volume, v_f , the thermodynamic diffusion coefficient, D_T , is given by [13]

$$D_T = \frac{RT}{\zeta} = RTA_D \exp\left(-\frac{B_D}{\phi_p v_f}\right) \quad (8)$$

where ϕ_p is the volume fraction of amorphous polymer, and

B_D and A_D depend on penetrant molecular size. A rather good approximation to the free volume is obtained from $v_f = [v_a(T) - v_c(T)]/v_a(T)$ where v_a and v_c are, respectively, the specific volumes of the amorphous and crystalline phases of LLDPE. Since the free volume is affected by pressure, temperature and amount of absorbed penetrant, the fractional free volume with respect to a reference state can be written as [14–17]

$$v_f(p, T, \phi_A) = v_f(p_r, T_r, 0) + \alpha_f(T - T_r) - \beta(p - p_r) + \gamma\phi_A \quad (9)$$

where the subindex r denotes the reference state and ϕ_A is the volume fraction of penetrant at the state defined by p and T . The parameters $\alpha_f = (\partial v_f / \partial T)_r$, $\beta = -(\partial v_f / \partial p)_r$ and $\gamma = (\partial v_f / \partial \phi_A)_r$ are positive constants that characterize the effectiveness of temperature, pressure and penetrant concentration for changing the free volume. The fractional free volume at constant temperature is the result of two at first sight opposing effects: the decrease of free volume, due to the hydrostatic pressure, and the increase in the value of v_f , caused by the sorption of the penetrant in the membrane. The results for the diffusion coefficient of CO₂, shown in Fig. 4, are not totally conclusive with respect to which of the two effects is dominant. It seems, however, that at high temperatures the sorption effect overcomes the compression effect in the diffusion of CO₂ in LLDPE membranes.

The rather sharp decrease in the apparent solubility coefficient of CO₂ observed at 50 and 60°C in Fig. 5, in the low pressures region, can be explained by means of the dual mode model. According to the model, the apparent solubility of CO₂ in LLDPE could be the result of Henry's solution, and trapped molecules in holes or microvoids located in crystal defects and/or crystalline–amorphous regions' interphases. Accordingly, the solubility coefficient can be written as [18,19]

$$S = k_D + \frac{bC'_H}{1 + bp} \quad (10)$$

where k_D is Henry's solution coefficient, C'_H the Langmuir sorption capacity and b is an affinity parameter characterizing the ratio of rate constants for sorption and desorption. These parameters can be obtained by plotting the results for S against $1/(1 + bp)$ for different values of b until a straight line is obtained. From the slopes and the intercepts of the straight lines of these plots, the values of k_D and bC'_H , respectively, are evaluated. The results for these parameters at 40, 50 and 60°C are shown in Table 1.

According to the dual mode theory [18,19], the diffusion of CO₂ in LLDPE membranes may occur by jumps of the dissolved molecules into non-permanent holes resulting from the micro-Browning motions of the chains in the amorphous phase (first mode), and partial mobility of the trapped molecules (second model) in the permanent holes. The dual-mode model leads to the following expression for the

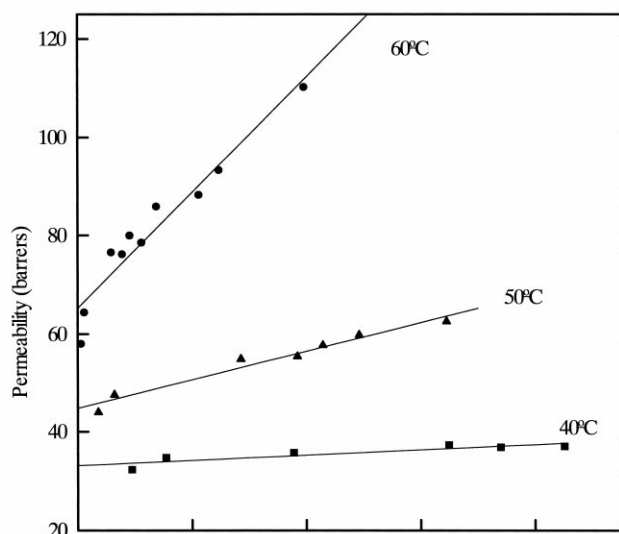


Fig. 8. Plot showing the fitting of values of the permeability coefficient of CO₂ to Eq. (11).

permeability coefficient:

$$P = k_D D_D + D_H \frac{b C'_H}{1 + bp} \quad (11)$$

where D_D and D_H are, respectively, the apparent diffusion coefficients for the sorbed molecules in the dissolved and trapped modes. The values of P at 40, 50 and 60°C, plotted as a function of $1/(1 + bp)$ in Fig. 8, fit to straight lines and the slopes and intercepts of which give, respectively, $k_D D_D$ and $b D_H C'_H$. These values, in conjunction with those corresponding to k_D and $b C'_H$ give D_D and D_H , the apparent diffusion coefficients for the sorbed molecules in the first and second modes, respectively. For comparative purposes, the values of the parameters of the dual mode model obtained in this work, together with those reported earlier for co-extruded LLDPE films [1–3], are shown in Table 2. An inspection of these results shows that the contributions of the first ($k_D D_D$) and second ($C'_H D_H$) modes to the perme-

Table 2

Parameters of dual mode for CO₂ in co-extruded (LLDPE_{co-ext}) and pressed (LLDPE_{press}) films

Parameters of dual mode	LLDPE _{co-ext}		LLDPE _{press}	
	$T = 45^\circ\text{C}$	40°C	50°C	60°C
b (cm Hg) ⁻¹	0.06	0.03	0.08	0.45
$10^3 \times k_D \text{ cm}^3$ of gas (STP)/(cm ³ of polymer cm Hg)	7.3	2.2	2.1	2.1
$C'_H \text{ cm}^3$ gas(STP)/cm ³ of polymer	0.53	0.23	0.18	0.12
$10^{10} \times k_D D_D$ (Barrers)	45.4	33.1	44.8	65.2
$10^{10} \times C'_H D_H \text{ cm}^3$ of gas (STP) cm/(cm ² s)	600	358	730	523
$10^7 \times D_D$ (cm ² /s)	6.2	15.1	21.7	31.2
$10^7 \times D_H$ (cm ² /s)	1.1	1.6	4.1	4.3

ability coefficient of CO₂ through polyethylene films as well as the affinity parameter (b) are of the same order for the co-extruded and pressed LLDPE films. More important differences are observed in the values of k_D and D_D which for co-extruded LLDPE are, respectively, one half and twice the respective values of these quantities for pressed LLDPE.

The co-extruded LLDPE films used in previous works [1–3] were also 1-octene-*co*-ethylene copolymers with roughly 8% mol content of the first comonomer. The films were made of three layers, i.e. C(15 wt%)A(70 wt%)B(15 wt%). A and C are Dowlex 2247 ($\rho = 0.902 \text{ g cm}^{-3}$) like that used in this study, and layer B is Dowlex 2291 ($\rho = 0.912 \text{ g cm}^{-3}$). The similarity of the transport of CO₂ in co-extruded and molded LLDPE films suggests that the microstructure developed in the films by the co-extrusion process, which so strongly affects the mechanical properties of LLDPE, hardly affects the transport of carbon dioxide through this material.

Whereas the diffusion coefficient obtained from permeation measurements is an average quantity given by

$$D = \frac{1}{C_h - C_l} \int_{C_l}^{C_h} D(C) dC \quad (12)$$

where C_h and C_l are, respectively, the concentration of the gas at the high and low pressure sides of the membrane, the concentration is kept constant throughout the sample in the determination of D using the NMR technique. The value obtained for the diffusion coefficient of CO₂ by permeation experiments under an upstream pressure of 9 atm is $6.86 \times 10^{-7} \text{ cm}^2 \text{ s}^{-1}$. This quantity is nearly one order of magnitude lower than the value of $5.65 \times 10^{-6} \text{ cm}^2 \text{ s}^{-1}$ found by NMR under a hydrostatic pressure of nearly the same magnitude. In principle, this discrepancy could be attributed to differences in morphology in the samples used, pellets in NMR and films in permeation. However, the fact that degree of crystallinity of the pellets and films was similar, specifically, 29 and 26%, respectively, seems to rule out this possibility. The explanation of the difference in the values of D obtained by the two techniques may lie in that NMR is an equilibrium measurement of self-diffusion whereas the permeation measurement is not an equilibrium measurement.

Earlier studies carried out on the dynamics of CO₂ in poly(dimethylsiloxane) rubber by NMR showed that the translational diffusion has a wide distribution [4,5]. From the spin–lattice and spin–spin relaxation times as well as nuclear Overhauser determined at three magnetic fields as a function of temperature, the diffusion coefficient of CO₂ in the silicone membrane was calculated finding that this parameter has a wide distribution. In fact, the values of the self-diffusion coefficient seem to span a range of nearly four orders of magnitude. Therefore, the value of D obtained in this work from NMR could be very well an average corresponding to the distribution of the diffusion coefficient of CO₂ in LLDPE.

As for the permeation measurements, the expression that

relates the permeability coefficient to the diffusion coefficient may not be a simple one. There are boundary effects [10] in the diffusion and non-linear concentration gradients in the sample that have to be accounted for. Moreover, in semi-crystalline membranes permeation will be limited only to the non-crystalline regions and the concentration will have to be scaled. All the effects involved in the determination of the diffusion coefficient by NMR and permeation measurements are difficult to analyze quantitatively. In most cases, however, trends between the diffusion coefficients obtained by NMR and permeation are similar, and one order of magnitude difference in the numbers is not unusual.

4. Conclusions

Transport of CO₂ in LLDPE films obtained by co-extrusion and compression experiences a high increase at moderately high temperatures as the upstream pressure p_h decreases, in the region of low values of p_h . This behavior is described by the dual-mode model finding that most of the parameters of the model are similar for both types of films.

The value of the diffusion coefficient of CO₂ in compressed films, determined by ¹³C NMR, is nearly one order of magnitude higher than that obtained from permeation measurements. This discrepancy seems to be too high to be attributed to the fact that the NMR measurement is an equilibrium measurement and the permeation is not. Other causes discussed in the text need to be investigated to explain the discrepancy observed.

References

- [1] Compañ V, Andrio A, López ML, Riande E. *Polymer* 1996;37:5831.
- [2] Compañ V, Andrio A, López ML, Alvarez C, Riande E. *Macromolecules* 1997;30:3317.
- [3] Compañ V, López ML, Andrio A, Riande E. *Macromolecules* 1998;31:6984.
- [4] Cain EJ, Jones AA, Inglefield PT, Jost RD, Liu X, Wen W-Y. *J Polym Sci: Part B: Polym Phys* 1990;28:1737.
- [5] Cain EJ, Wen W-Y, Jones AA, Inglefield PT, Cauley BJ, Bendler JT. *J Polym Sci: Part B: Polym Phys* 1991;29:1009.
- [6] Carslaw HS, Haeger L. *Conduction of heat in solids*. Oxford: Oxford University Press, 1959 (p. 213).
- [7] Crank J. *The mathematics of diffusion*. Oxford: Oxford University Press, 1975.
- [8] Barrer RM. *Trans Faraday Soc* 1939;35:628.
- [9] Zupancic I, Lahajnar G, Blinc R, Reneker DH, Peterlin A. *J Polym Sci Polym Phys Ed* 1978;16:1399.
- [10] Stejskal EO, Tanner JE. *J Chem Phys* 1965;42:288.
- [11] Flory PJ. *Principles of polymer chemistry*. Ithaca: Cornell University Press, 1953 (chap. 21).
- [12] Petropoulos JH. *Pure Appl Chem* 1993;65:219.
- [13] Fujita H. *Adv Polym Sci* 1961;3:1.
- [14] Fujita H, Kishimoto A, Matsumoto K. *Trans Faraday Soc* 1960;56:424.
- [15] Stern SA, Fang SM, Frisch HL. *J Polym Sci: Part A-2* 1972;10:201.
- [16] Fang SM, Stern SA, Frisch HL. *Chem Engng Sci* 1975;30:773.
- [17] Kulkarni SS, Stern SA. *J Polym Sci: Polym Phys Ed* 1983;30:441 (see also p. 467).
- [18] Michaels A, Vieth WR, Barrie JA. *J Appl Polym Sci* 1963;34:1.
- [19] Kesting RE, Fritzsche AK. *Polymeric gas separation membranes*. New York: Wiley, 1993 (chap. 3, p. 60).